BIOCHEMISTRY AND MOLECULAR BIOLOGY EDUCATION
Vol. 33, No. 5, pp. 335–343, 2005

Articles

A Docking Interaction Study of the Effect of Critical Mutations in Ribonuclease A on Protein-Ligand Binding

Received for publication, May 25, 2004, and in revised form, February 8, 2005

Sayan Mukherjee, Soumya De‡, Zhumur Ghosh§, and Swagata Dasgupta¶

From the Department of Chemistry, Indian Institute of Technology, Kharagpur 721 302, India

Enzymes with ribonucleolytic activity play a pivotal role in gene expression and cellular homeostasis by altering the levels of cellular RNA. Ribonuclease A has been the most well studied of such enzymes whose histidine residues (His^{12} and His^{119}) play a crucial role in the catalytic mechanism of the protein. The ligands chosen for this study, 2′CMP and 3′CMP, act as competitive substrate analog inhibitors of this enzyme. Using molecular graphics software freely available for academic use, AutoDock and PyMol, we demonstrate that substitution of either histidine residue by alanine causes marked changes in the distances between these critical residues of the enzyme. The ligands in the docked conformation (particularly on mutation of His^{119} to Ala) compensate for the altered free energy and hydrogen bonding abilities in these new protein-ligand complexes.

Keywords: Docked conformation, substrate analog inhibitors, molecular graphics, hydrogen bonding, free energy, protein-ligand complexes.

Ribonuclease A (RNase A[1]; EC 3.1.27.5) has been one of the most studied enzymes of the last century, including the landmark 1957 Anfinsen experiment demonstrating beyond doubt, for the first time, the cardinal importance of amino acid sequence on the eventual shape of the folded protein. Crystallized more than 50 years ago and the first enzyme for which a correct amino acid sequence was determined, RNase A was the third enzyme for which the three-dimensional (3D) structure was determined [1].

Pioneering work relating to protein chemistry and enzymology has been accomplished with RNase A (Fig. 1). The predominant form of the enzyme present in bovine pancreas has been suffixed with an "A" in its name [2]. Renewed interest in this protein in the past decade has been due to a large number of ribonuclease-type enzymes exhibiting unusual biological activities [2–6]. Cellular RNA levels are controlled post-transcriptionally by ribonucleases of varying specificity. Angiogenin, neurotoxins, and plant allergens are among the myriad of proteins with RNase activity or significant homology to known RNases. RNases are regulated by specific activators and inhibitors, both natural and synthetic, including interferons and diet-derived plant polyphenols and are thus potential targets for the development of small and simple ligands as therapeutic interventions in such widespread diseases.

The enzyme catalyzes the cleavage of RNA via a cyclic phosphate intermediate. In this enzyme, two histidines are located near the bond to be cleaved. In the cyclization step, His^{12} acts as a general base catalyst and His^{119} as a general acid catalyst (His^{12} and His^{119} in bovine pancreatic ribonuclease). These roles are reversed in the step involving hydrolysis of the cyclic phosphate intermediate (Fig. 2) [6].

DNA lacks the hydroxyl group at the 2′ position essential for the formation of the cyclic intermediate and hence is not cleaved by ribonuclease. The ribonuclease molecule has a well defined binding cleft that comprises a ribose-binding site, a phosphate-binding site (P), and a base-binding site (B), as shown in Fig. 3.

Here we demonstrate the effect of mutation of each of the aforementioned His residues on the binding of competitive inhibitors 2′-cytidine monophosphate (CMP) and 3′CMP. To accomplish this, we have used a docking procedure that is used extensively in computer-aided drug design. Macromolecular crystallography provides us with the three-dimensional structure of large biomolecules, the knowledge of which is essential for a complete understanding of its function. Docking studies have become one of the most useful applications of this technique. The basic feature of docking is to identify the site of interaction of potential drug candidates to a target macromolecule [7]. The structure of the drug, its receptor, and the interactions between them are analyzed closely to find the best way to optimize geometry and activity or to give an indication of which molecules would be the most interesting to synthesize [8, 9].

‡ Current address: Dept. of Chemistry and Chemical Biology, Cornell University, Ithaca, NY 14853.

§ Current address: Dept. of Theoretical Physics, Indian Association for the Cultivation of Science, Kolkata 700 032, India.

¶ To whom correspondence should be addressed. Fax: 91-3222-255303; E-mail: swagata@chem.iitkgp.ernet.in.

[1] The abbreviations used are: RNase A, ribonuclease A; CMP, cytidine monophosphate; PDB, Protein Data Bank; 3D, three dimensional. GUI, graphical user interface; ADT, AutoDockTools.

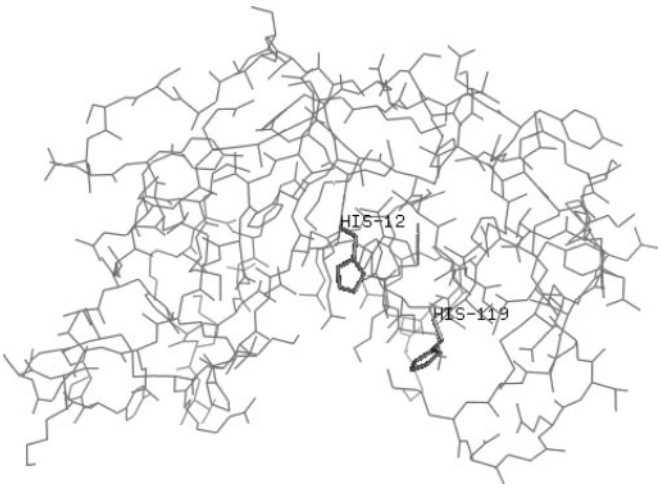

FIG. 1. **Structure of wild-type RNase A (PDB filename 1FS3.pdb).** The His^{12} and His^{119} residues have been labeled.

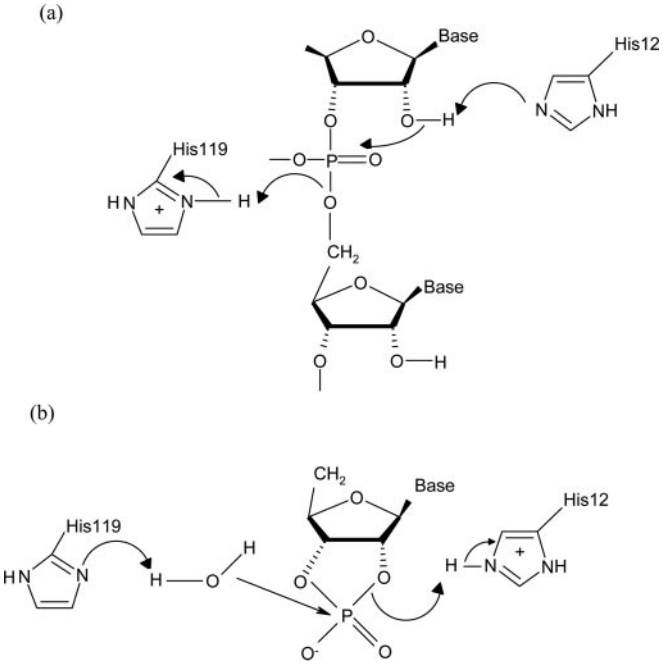

FIG. 2. **Mechanism of action of RNase A.** *a*, cyclization step: His^{12} acts as the base and His^{119} as the acid. *b*, hydrolysis step: The roles of the His residues are reversed.

MATERIALS AND METHODS

Materials

All software used for this analysis is free for academic use. The simple approach gives an insight into the basic use of different molecular graphics software presently in use and how further analysis may be possible. A list of the sites from where data/software has been obtained is provided below followed by a short description of what is available.

The Protein Data Bank (www.rcsb.org) [10]—The Protein Data Bank (PDB) is a worldwide repository for the processing and distribution of 3D biological macromolecular structure data. Presently it has more than 25,000 structures determined by x-ray diffraction. Protein structures may be downloaded from the site with specific keywords or a PDB alphanumeric filename.

PyMol (Version 0.97, Delano Scientific, 2004, www.pymol.org) [11]—PyMol is a Python-based visualization software. The files of the proteins obtained from the PDB can be visualized using PyMol. It has tools for measuring distances as well as identifying

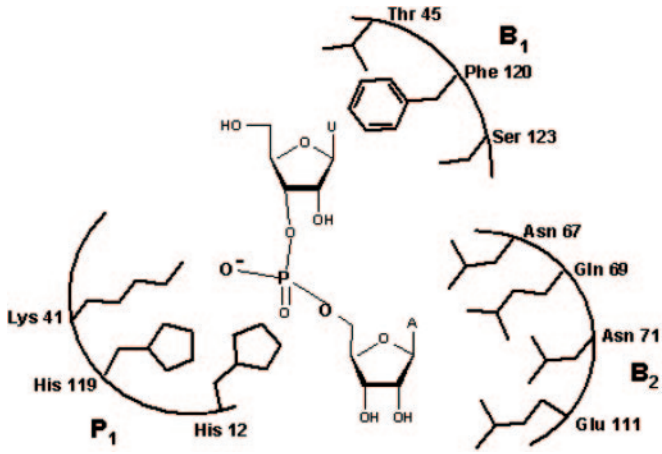

FIG. 3. **Schematic diagram depicting the amino acid residues in the binding pockets of RNase A.** *P* and *B* represent the phosphate- and base-binding sites, respectively.

different atoms. PyMol has been selected for the analysis of the docking results.

AutoDock (Version 3.0, The Scripps Research Institute, www.scripps.edu) [12, 13]—The docking experiments were performed using the docking software AutoDock 3.0 with the help AutoDockTools, an accessory program that allows the user to interact with AutoDock from a graphic user interface (GUI). AutoDock is a suite of automated docking tools designed to predict how small molecules/ligands, such as substrates or drug candidates, bind to a receptor/protein of known 3D structure. AutoDock (version 3.0) consists of three separate programs: AutoDock, which performs the docking of the ligand to a set of grids describing the target protein; AutoGrid, which precalculates these grids; and AutoTors, which sets up which bonds will be treated as rotatable in the ligand.

Preparation of the Macromolecule and Ligand Files for AutoDock

Using the GUI of AutoDockTools (ADT) we prepared the files as follows.

The Macromolecule File—The downloaded PDB files were first read in ADT, added waters were removed, and polar hydrogens were added. ADT then checked if the molecule had charges, and if not it added Kollman charges [by default; ADT adds Kollman charges for a peptide (determined by checking whether all of its component residue names appear in the standard set of 20 commonly occurring amino acids) and Gasteiger charges if not so]. Finally, solvation parameters were added and the files saved as molecule.pdbqs (where "q" and "s" represent charge and solvation, respectively).

The Ligand File—In a similar procedure, the ligand files were read in ADT, nonpolar hydrogens were merged, and charges were added. ADT then determined the best root (the best root is the atom in the ligand with the smallest or largest subtree; in case of a tie, if either atom is in a cycle, it is picked as the root, and if neither or both is in a cycle, the first found is picked). Next we defined rotatable bonds in the ligand, making all amide bonds nonrotatable, and set the number of active torsions to fewest atoms. The ligand file was then saved with a ligand.out.pdbq extension ("q" representing charge).

Preparation of the Grid Parameter File—For the calculation of docking interaction energy, it is necessary to create a 3D box (grid) in which the protein molecule is enclosed. The grid volume should be large enough to allow the ligand to rotate freely, even when the ligand is in its most fully extended conformation. The parameters required to create such a grid are stored in the grid parameter file, molecule.gpf. The autogrid3 job was then run

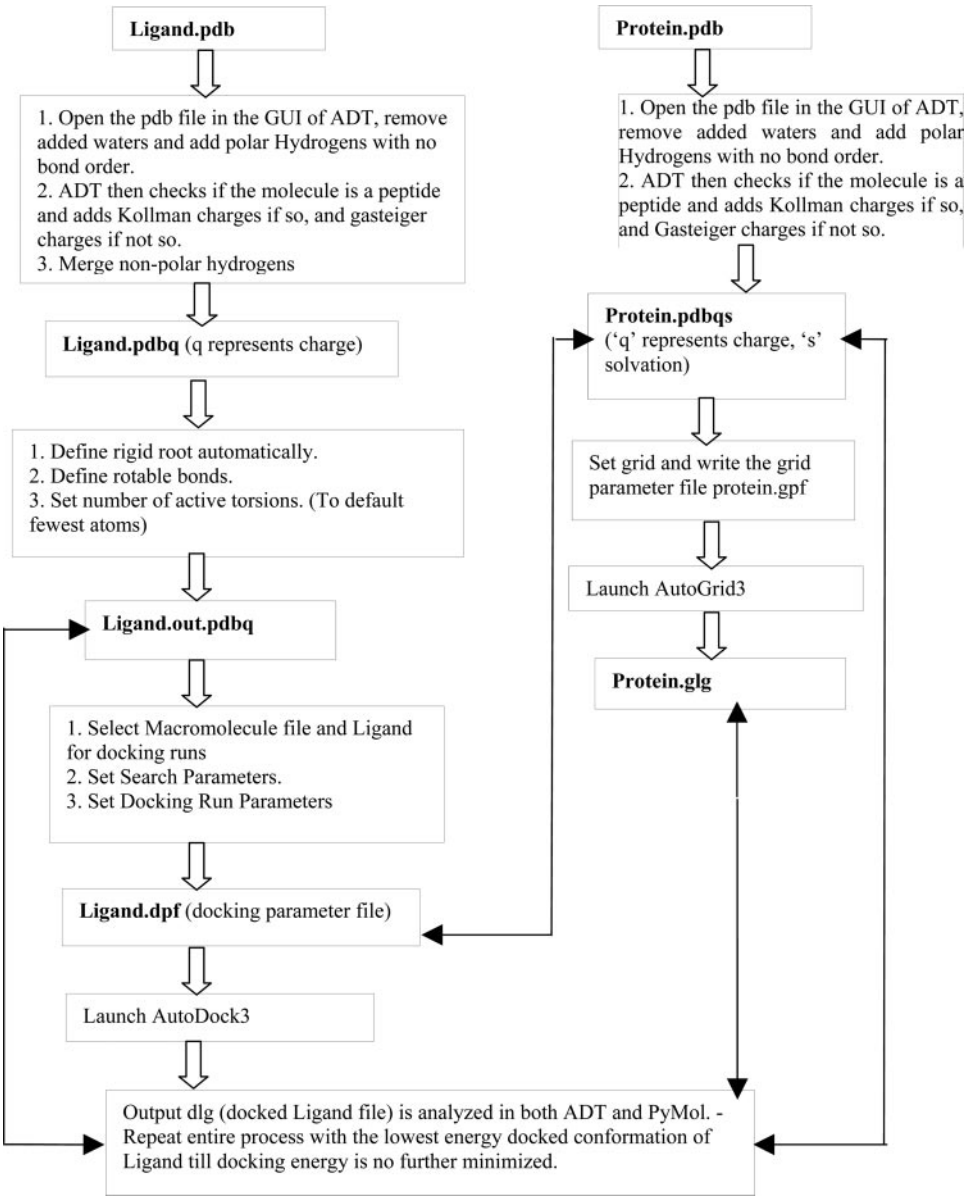

FIG. 4. **Schematic diagram of the procedure.**

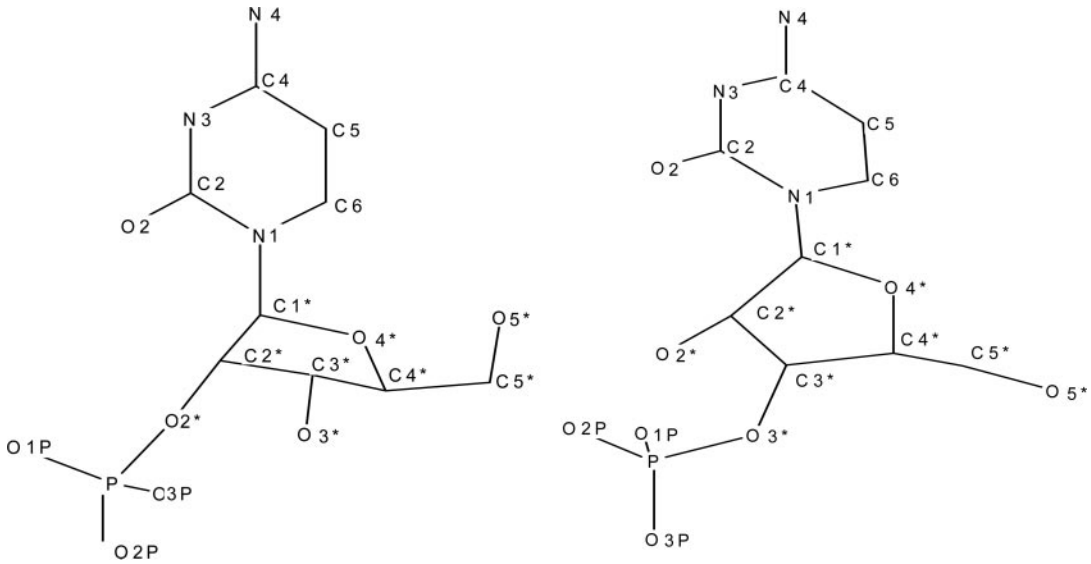

FIG. 5. **Labeling schemes for the ligands 2′CMP (*left*) and 3′CMP (*right*).**

to create a map for every atom type in the ligand and create the corresponding macromolecular file with the extension molecule.glg.

Preparation of Docking Parameter File—The docking parameter file, which instructs AutoDock about the ligand to move, the map files to use, and other properties defined for the ligand, was created. The search methods of AutoDock include the Monte Carlo simulated annealing method, the genetic algorithm, local search, and the hybrid genetic algorithm with local search. The latter is also referred to as the Lamarckian genetic algorithm because offsprings are allowed to inherit the local search adaptations of their parents, and this was the chosen algorithm for the analysis.

Finally the autodock job was run from the GUI of ADT, and the docked ligand files (.dlg extension) were used for study. The .dlg files were read in ADT as well as in PyMol to calculate the interatomic distances in the docked ligand-protein complexes. The entire procedure is given below in the flowchart (Fig. 4).

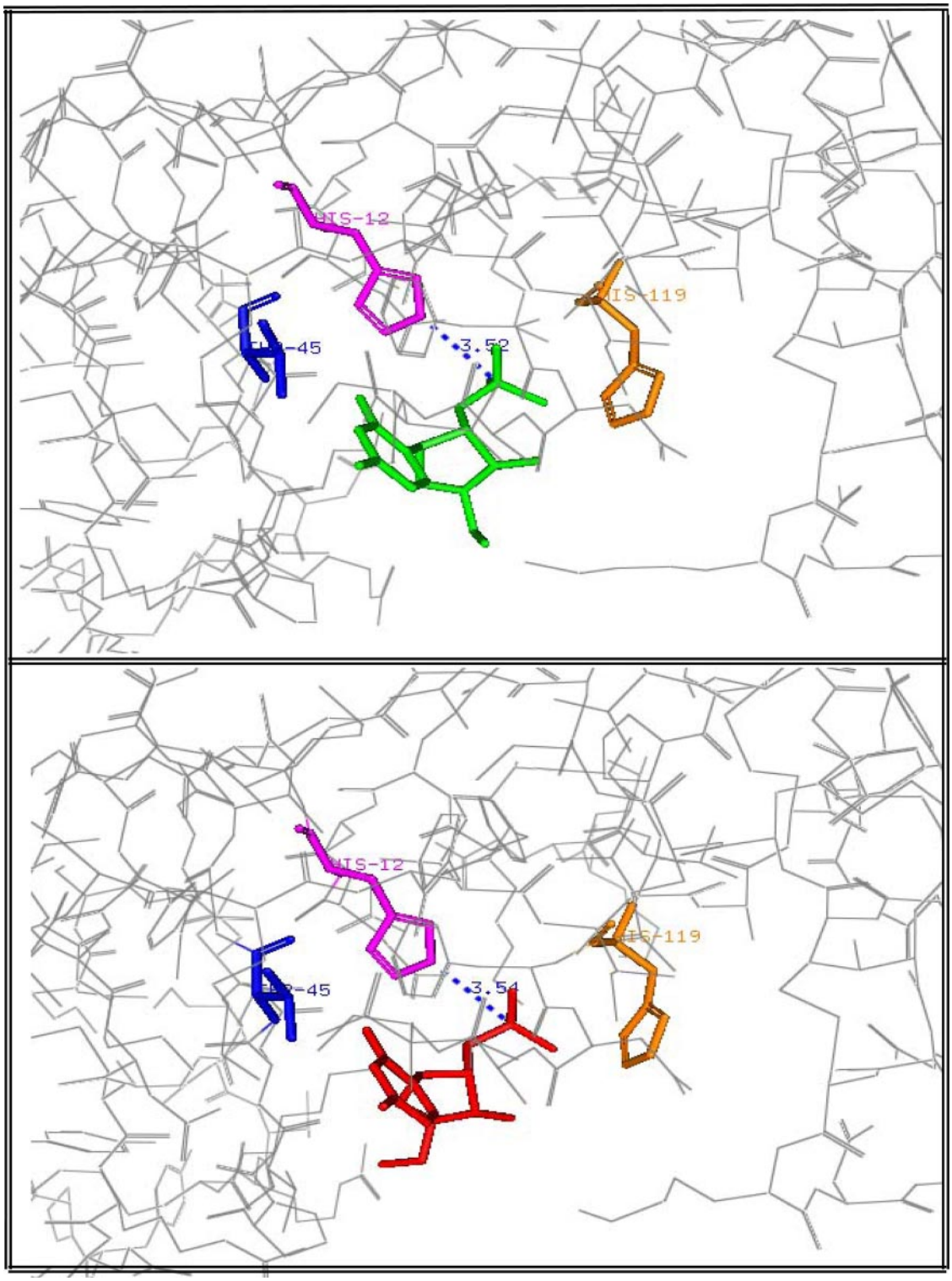

FIG. 6. **The *top panel* represents 2′CMP (*green*) complexed with RNase A (1JVU from the PDB), and the *bottom panel* shows the ligand (*red*) docked onto 1FS3 using AutoDock.** Both macromolecules are in same orientation, and the active site residues Thr^{45}, His^{12}, and His^{119} have been highlighted. The His^{12} (NE2)-C-2-P (P) distances are shown for comparison.

RESULTS AND DISCUSSION

The docked conformation of 2′CMP onto 1FS3 (wild-type RNase A) shows marked resemblance in orientation and distances with neighboring residues in the active site pocket of the enzyme with that reported in the PDB as 1JVU (2′CMP complexed with wild-type RNase A) (Fig. 5). Being a competitive inhibitor, 2′CMP docks onto the active site pocket of the protein and hydrogen bonding becomes possible with nearby residues Thr^{45}, His^{12}, and His^{119}.

Our results are further consolidated by 3′CMP, which docks comparatively weakly onto 1FS3, albeit still in the active site cavity (final docked energy = –9.38 kcal/mol compared with –10.72 kcal/mol for 2′CMP), when its orientation and interresidue distances are compared with 1RPF (the reported structure in the PDB of 3′CMP complexed with wild-type RNase A). The root mean square deviation of superposed structures of 1FS3 (wild type) with docked 2′CMP and 1JVU (from the PDB) was only 0.014 (Fig. 6).

Marked changes occur on mutating the active site histidines (His^{12} and His^{119}) to alanine in terms of orientation of the ligand in the protein-ligand docked complex. In 1C9V (His^{12} mutated to Ala), the docking of 2′CMP is weakened, and final docked energy is reduced (less negative). The two possible orientations of His^{119} reported in 1C9V.pdb are situated about 5 and 4 Å further away than in 1FS3 in terms of the His^{119} (ND1)-C-2′-P (O1P) (our numbering scheme is illustrated in Fig. 5) distance in their proximal and distal stereochemistries, respectively. Interestingly, the orientation of the ligand is such that the His^{119} (ND1)-C-2′-P (O2P) distances (not shown in Table I) are a bit shorter than the His^{119} (ND1)-C-2′-P (O1P) distances, the former being 6.47 and 5.68 Å (proximal and distal histidines) and the latter 8.88 and 8.03 Å, respectively. The substituted Ala^{12} residue of course has its β carbon closer than the β carbon of the original His residue, owing to the absence of the imidazole ring of histidine.

The phosphate-recognition site P1 of the wild-type enzyme has His^{119} oriented in a direction opposite to that of 1C9V. This feature has affected the binding of the ligand to the active site region, which is reflected in the measurement of distances between, and the ligand and these residues (Table I), implying that the absence of His^{12} at the phosphate-binding site significantly alters ligand conformation. At the same time, Thr^{45} (N)-C-2′-P (O_2) and Thr^{45} (OG1)-C-2′-P (N3) distances are more or less conserved in 1C9V, implying that the base-binding site is not affected (Fig. 7).

Distinctive changes occur on mutation of the His^{119} residue to Ala (1C9X) with the final docked energy being –7.16 kcal/mol, an increase of 3.56 kcal/mol. The stereochemistry of the docked ligand shifts from the active site pocket, the Thr^{45} (N)-C-2′-P (O_2) and Thr^{45} (OG1)-C-2′-P (N3) distances increasing more than 2-fold to 6.01 and 5.47 Å, respectively (Fig. 6). Concurrently, the His^{12} (NE2)-C-2′-P (O1P) and His^{12} (CB)-C-2′-P (P) distances remain relatively conserved as in the wild-type form (the latter elongated to 4.4 Å), suggesting that the absence of His^{119} at the phosphate-binding site greatly alters ligand stereochemistry, but the phosphate-binding site is not affected significantly (Fig. 7).

When 3′CMP is chosen as the ligand, the root mean square deviation of superposed structures of 1FS3 (wild type) with 3′CMP docked and 1RPF was 0.033. The already weaker binding is altered to a smaller extent on mutating His^{12} to Ala (1C9V), and in fact the absence of the His^{12} residue facilitates 3′CMP binding to a small extent as reflected in a slightly greater docking energy (more negative), plausibly to accommodate for altered hydrogen bonding and free energy conditions (Fig. 8). However, similar trends in internuclear distances occur as for 2′CMP, that is increased His^{119} (ND1)-C-3′-P (O1P) distances by about 2–3 Å with proximal and distally oriented His^{119} and conservation of Thr^{45} (N)-C-3′-P (O2) and Thr^{45} (OG1)-C-3′-P (N3) lengths (slight increase). As in 2′CMP, binding of the ligand is drastically weakened in terms of the final docked energy in 1C9X, 3′CMP having a value of

TABLE I

Comparison of critical distances of residues in docked conformation of 2′CMP and 3′CMP on RNase A (wild-type 1FS3 and mutants 1C9V [His^{12} to Ala]) and 1C9X [His^{119} to Ala]) obtained using AutoDock, with reported values in the PDB (1JVU and 1RPF, respectively) [all distances in angstroms]

PDB ID	Final docked energy	Thr^{45} (N) C-2′-P (O2)	Thr^{45} (OG1) C-2′-P (N3)	His^{12} (NE2) C-2′-P (O1P)	His^{12} (CB)-C-2′-P (P)	His^{119} (ND1)-C-2′P (O1P)	His^{119} (CB) C-2′-P (P)
	kcal/mol						
2′CMP							
1FS3[a]	–10.72	2.67	2.58	2.70	7.14	3.84	5.02
1JVU (reported)	–	2.82	2.63	2.56	7.15	3.87	4.76
1C9V (His^{12} to Ala)						a)8.88	a)5.39
	–10.20	2.73	3.03	–	4.19[b]	b)8.03	b)5.54
1C9X (His^{119} to Ala)	–7.16	6.01	5.47	4.40	7.04	–	5.22[b]
3′CMP							
1FS3[c]	–9.38	2.66	3.08	4.64	8.27	3.83	4.39
1RPF (reported)	–	2.72	2.89	4.66	7.63	3.24	4.36
1C9V (His^{12} to Ala)						a)6.54	a)5.51
	–10.50	3.01	3.65	–	4.06	b)5.33	b)5.67
1C9X (His^{119} to Ala)	–8.13	6.03	4.56	2.93	6.96	–	5.18[b]

[a] Final docked energy, –10.72 kcal/mol; final intermolecular energy, –10.79 kcal/mol; estimated K_i, +1.01e-07; final internal energy of ligand, +0.06 kcal/mol.

[b] Distances with corresponding alanine residue.

[c] Final docked energy, –9.38 kcal/mol; final intermolecular energy, –9.32 kcal/mol; estimated K_i, +1.2e-06; final internal energy of ligand, –0.05 kcal/mol.

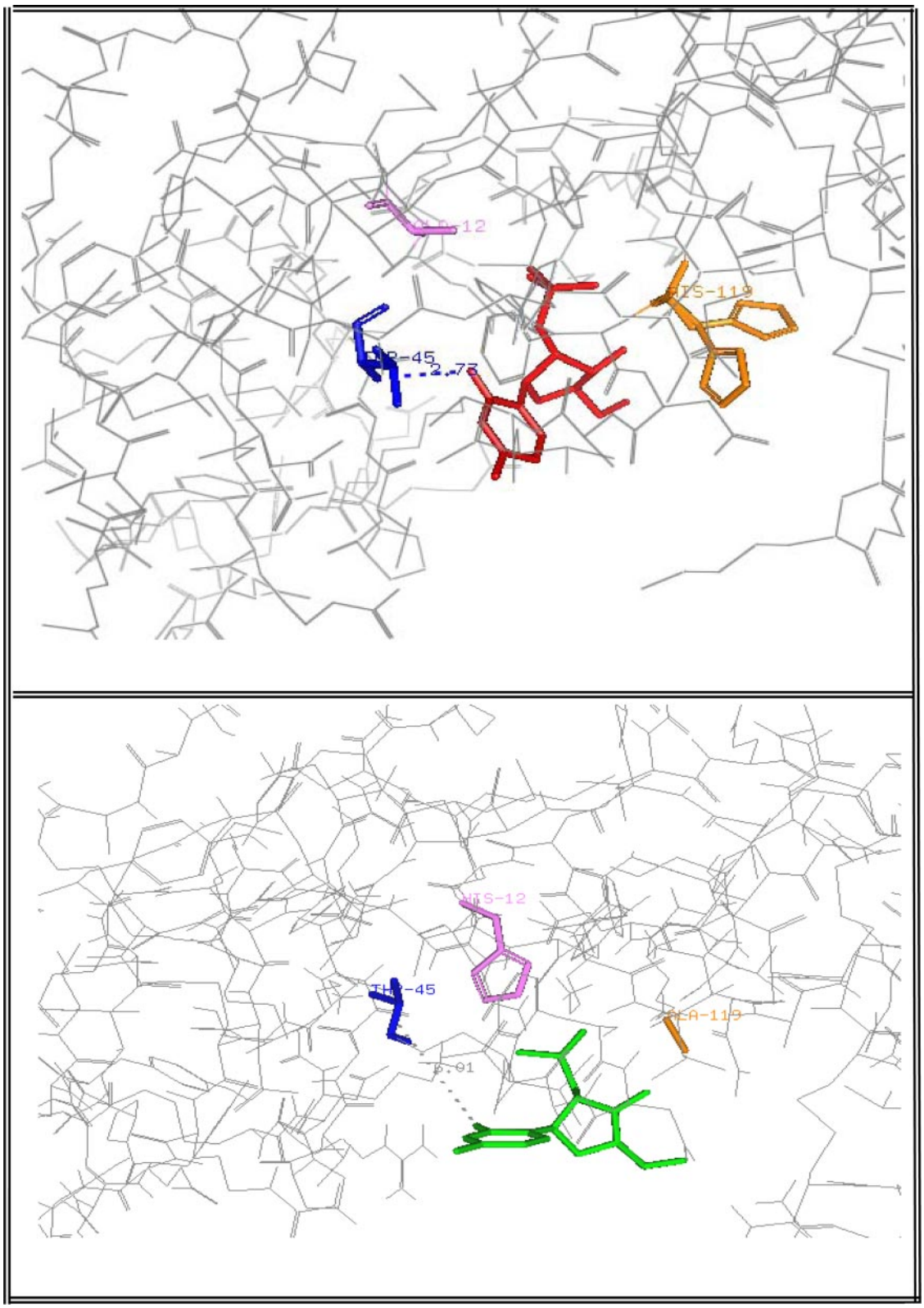

FIG. 7. **The *top panel* shows the ligand 2′CMP docked onto 1C9V (*red*), and the *bottom panel* shows the legend docked onto 1C9X (*green*).** In both cases, the macromolecules are orientated as in Fig. 5, the same residues are highlighted (Thr^{45}, His^{12}, His^{119}), and the Thr^{45} (N)-C-2-P (O2) distances are marked for comparison.

−8.13 kcal/mol. In this docked protein (1C9X)-3′CMP complex, Thr^{45} (N)-C-3′-P (O2) and Thr^{45} (OG1)-C-3′-P (N3) distances increase nearly 2-fold to 6.03 and 4.56 Å, respectively, although His^{12} (NE2)-C-3′-P (O1P) and His^{12} (CB)-C-3′-P (P) distances remain intact, rather than decrease to a small degree to accommodate for the changes in hydrogen bonding and molecular energy constraints, as compared with the wild-type enzyme (Fig. 9). In this context, His^{12} (NE2)-C-3′-P (O1P) and His^{12} (NE2)-C-3′-P (O3P) distances decrease to 2.93 and 2.83Å, respectively.

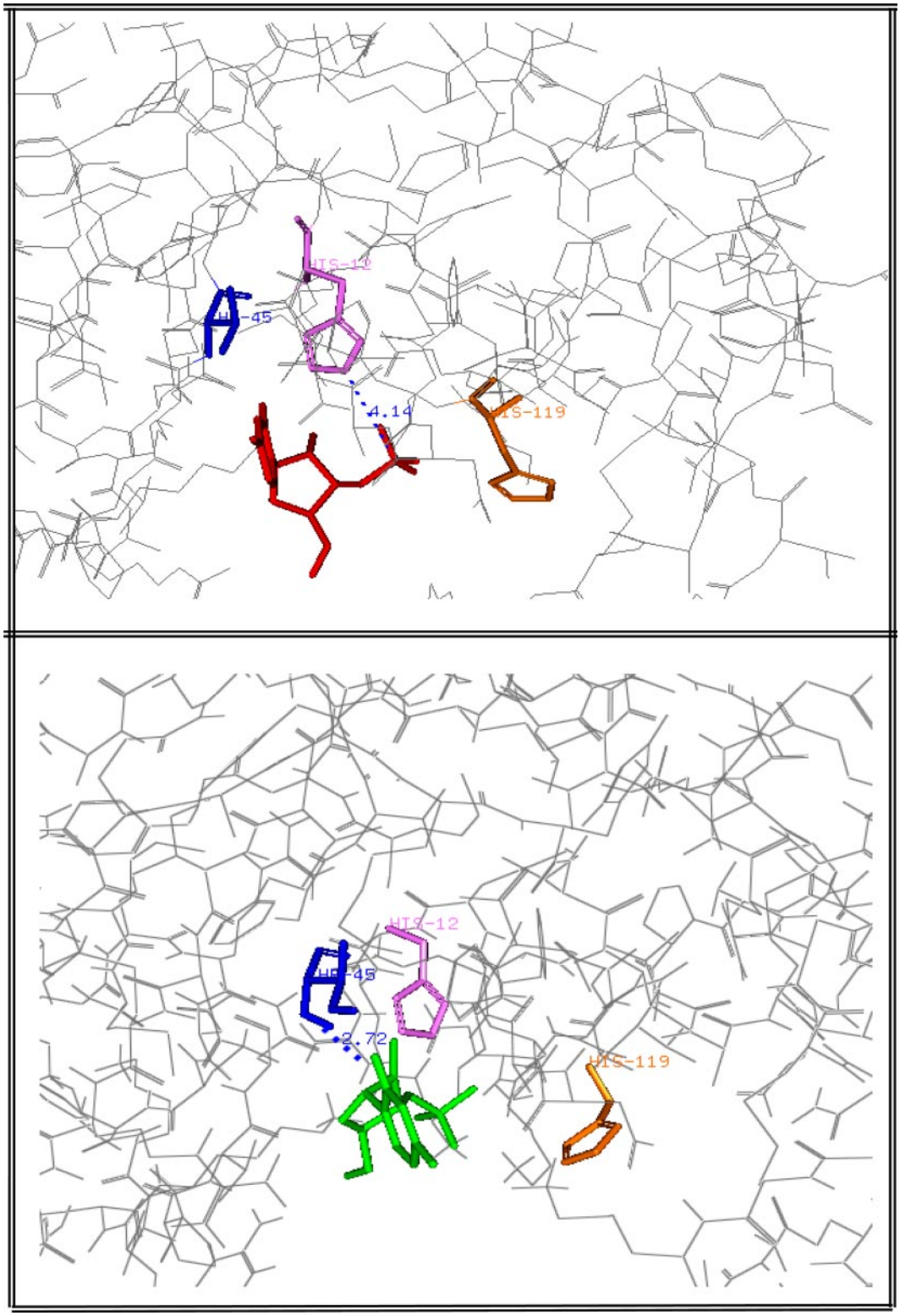

FIG. 8. **The *top panel* shows the ligand 3′CMP (*red*) complexed with RNase (1RPF from the PDB), and the *bottom panel* 3′CMP (*green*) docked onto the active site residues Thr^{45}, His^{12}, and His^{119} have been highlighted; the His^{12} (NE2)-C-2-P (P) distances are shown for comparison.**

CONCLUSION

The docking results as consolidated by comparison with reported protein-ligand complexes from the PDB demonstrate the relative accuracy and ease of using molecular graphics software like AutoDock. Mutations in critical active site histidines of RNase A has marked implications for substrate analog inhibitor/ligand bindings of 2′CMP and 3′CMP as indicated by significant changes of docking energy and interatomic distances in the protein-ligand docked complexes.

The absence of His^{12} orients the His^{119} in the opposite direction, which shifts the phosphate away from the His^{119}

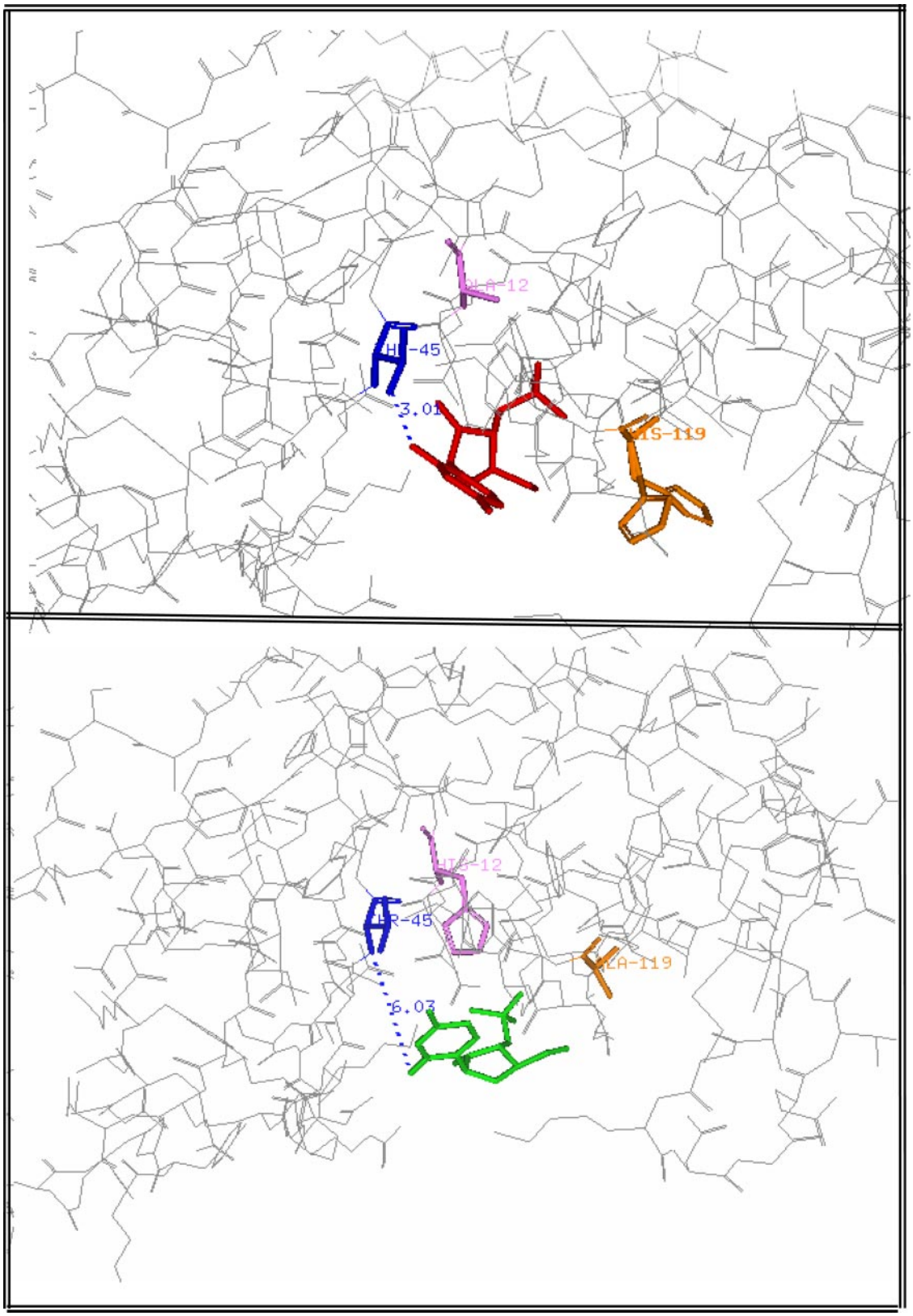

FIG. 9. **The *top panel* shows the ligand 3′CMP docked onto 1C9V (*red*), and the *bottom panel* shows the ligand docked onto 1C9X (*green*).** In both cases, the macromolecules are orientated similarly, and the same residues are highlighted (Thr^{45}, His^{12}, His^{119}); the Thr^{45} (N)-C-2-P (O2) distances have been marked for comparison.

residue. This implies that the change in His^{12} by Ala^{12} affects the phosphate-binding site of the ligand, whereas the base-binding site remains unaffected. Again, the absence of His^{119} shifts the six-membered ring of the base (ligand) away from Thr^{45}, hence reducing the interaction with it, whereas the phosphate remains at a proximal distance from His^{12}. This implies that the change in His^{119} by Ala^{119} affects the base-binding site, whereas the phos-

phate-binding site remains unaffected.

This exercise provides an opportunity to explore the docking procedure and compare the results obtained with actual crystal structures available in the PDB. Our analysis here is a simple demonstration of a generalized scheme widely applicable to structural bioinformatics for docking and model development in therapeutic drug design.

REFERENCES

[1] D. Voet, J. G. Voet (1995) *Biochemistry*, 2nd Ed., John Wiley & Sons, New York.

[2] G. D'Alessio (1993) New and cryptic biological messages from RNases, *Trends Cell Biol.* **3**, 106–109.

[3] C. H. Schein (1997) From housekeeper to microsurgeon: The diagnostic and therapeutic potential of ribonucleases, *Nat. Biotechnol*. **15**, 529–536.

[4] J. F. Riordan, Structure and function of angiogenin, in G. D'Alessio, J. F. Riordan, eds. (1997) *Ribonucleases: Structures and Functions*, pp. 445–489, New York.

[5] R. T. Raines (1998) Ribonuclease A, *Chem. Rev.* **98**, 1045–1065.

[6] G. D'Alessio, A. Di Donato, L. Mazzarella, R. Piccoli, in G. D'Alessio, J. F. Riordan, eds. (1997) Seminal ribonuclease: The importance of diversity, in *Ribonucleases: Structures and Functions*, pp. 383–423, New York.

[7] G. M. Morris, D. S. Goodsell, R. S. Halliday, R. Huey, W. E. Hart, R. K. Belew, A. J. Olson (1998) Automated docking using a Lamarckian genetic algorithm and an empirical binding free energy function, *J. Computational Chemistry* **19**, 1639–1662.

[8] D. D. Leonidas, G. B. Chavali, N. G. Oikonomakos, E. D. Chrysina, M. N. Kosmopoulou, M. Vlassi, C. Frankling, K. Ravi Acharya (2003) High-resolution crystal structures of ribonuclease A complexed with adenylic and uridylic nucleotide inhibitors. Implications for structure-based design of ribonucleolytic inhibitors, *Protein Sci.,* **12**, 2559–2574.

[9] D. M. Smith, K. G. Daniel, Z. Wang, W. C. Guida, T.-H. Chan, Q. P. Dou (2004) Docking studies and model development of tea polyphenol proteasome inhibitors: Applications to rational drug design, *Proteins Struct. Funct. Bioinform.* **54**, 58–70.

[10] H. M. Berman, J. Westbrook, Z. Feng, G. Gilliland, T. N. Bhat, H. Weissig, I. N. Shindyalov, P. E. Bourne (2000) The Protein Data Bank, *Nucleic Acids Res.* **28**, 235–242.

[11] W. L. Delano (2004) *The PyMol Molecular Graphics System*, Delano Scientific, San Carlos, CA.

[12] R. Huey, G. M. Morris (2003) *Using AutoDock with AutoDockTools: A Tutorial*, The Scripps Research Institute, Molecular Graphics Laboratory, La Jolla, CA.

[13] G. M. Morris, D. S. Goodsell, R. Huey, W. E. Hart, S. Holliday, R. Belew, A. J. Olson (2001) *User's Guide AutoDock: Automated Docking of Flexible Ligands to Receptors*, The Scripps Research Institute, Molecular Graphics Laboratory, La Jolla, CA.